CFD Simulation of Surface-to-Bed Heat Transfer in a Freely Bubbling Fluidized Bed

Azmat Mahmood, Dahai Zhang, Murat Koksal*
Mechanical Engineering Department, Dalhousie University
5269 Morris Street, B3J 1B6, Halifax, Canada
*to whom the correspondence should be addressed
e-mail: Murat.Koksal@dal.ca

Abstract
2-D CFD simulations were carried out to model the surface-to-bed heat transfer in a laboratory scale bubbling fluidized bed (0.17 m ID) with glass bead particles. A commercial CFD software, FLUENT V6.2, was used in the simulations. The multiphase flow model was a granular two-fluid (Eulerian-Eulerian) approach with kinetic theory of granular solids for the particle phase stresses. The simulation results were compared with the experimental data obtained from the bubbling fluidized bed. The results showed that the simulated heat transfer coefficients were sensitive to the modeling of solids phase thermal conductivity. The number of computational cells and particle-particle coefficient of restitution were found to affect the overall heat transfer coefficient.

Introduction

With the rapid development in computer technology, Two-Fluid (TF) approach has become a viable tool for modeling the transport phenomena in fluidization systems. Most studies using TF approach have concentrated on modeling the gas-solid hydrodynamics in fluidized beds and there are only a few studies pertinent to the application of TF approach to model the surface-to-bed heat transfer in bubbling fluidized beds [1-5]. Syamlal and Gidaspow [1] and Kuipers et al. [2] modeled the wall-to-bed heat transfer considering a bubbling fluidized bed kept at minimum fluidization conditions while a jet of gas was injected near a heated isothermal wall. Schmidt et al. [3,4] modeled the heat transfer between an immersed cylindrical isothermal surface and the bubbling bed using FLUENT. Recently, Patil et al. [5] showed that the heat transfer predictions with TF model could be substantially improved by incorporating an empirical porosity profile near the wall. In this paper, we report the results of TF simulations of heat transfer from an immersed cylindrical cartridge heater to a freely bubbling fluidized bed of glass bead particles. The simulations were carried by a commercial CFD package, FLUENT v6.2. The simulated time averaged HTCs were compared with those obtained from experiments and crucial parameters affecting the simulation results were identified.

Model Equations

We follow a TF formalism with kinetic theory of granular solids for the stresses in the particle phase (Table 1). Each phase is characterized by its own mass, momentum and energy conservation equations [9] with the following assumptions: the gas phase is incompressible and particles are perfectly spherical and mono-sized. The solids shear and bulk viscosities, and pressure (parameters needed to close the solids phase stress tensor) are determined based on the kinetic theory of granular solids applied to fluidization [9, 10]. In this context, it is suggested that individual particle velocity fluctuations, which are mainly due to particle-particle collisions and particle-gas interactions, generate an effective pressure and viscosity forming the stresses in the solids assembly.

Table 1. Conservation Equations

Conservation of mass for gas and solids phases	$\frac{\partial}{\partial t}\left(\alpha_g \rho_g\right) + \nabla.\left(\alpha_g \rho_g \vec{u}_g\right) = 0$	(1)
	$\frac{\partial}{\partial t}\left(\alpha_s \rho_s\right) + \nabla.\left(\alpha_s \rho_s \vec{u}_s\right) = 0$	(2)
Conservation of momentum for gas and solids phases	$\frac{\partial}{\partial t}\left(\alpha_g \rho_g \vec{u}_g\right) + \nabla.\left(\alpha_g \rho_g \vec{u}_g \vec{u}_g\right) = -\alpha_g \nabla p + \nabla.\overline{\overline{\tau}}_g + \alpha_g \rho_g \vec{g} + K_{gs}\left(\vec{u}_g - \vec{u}_s\right)$	(3)
	$\frac{\partial}{\partial t}\left(\alpha_s \rho_s \vec{u}_s\right) + \nabla.\left(\alpha_s \rho_s \vec{u}_s \vec{u}_s\right) = -\alpha_s \nabla p - \nabla p_s + \nabla.\overline{\overline{\tau}}_s + \alpha_s \rho_s \vec{g} + K_{gs}\left(\vec{u}_s - \vec{u}_g\right)$	(4)
Gas and solid phase stress tensors using Newtonian stress-strain relation	$\overline{\overline{\tau}}_g = \mu_g\left[\nabla \vec{u}_g + \left(\nabla \vec{u}_g\right)^T\right]$	(5)
	$\overline{\overline{\tau}}_s = \left(\zeta_s - \frac{2}{3}\mu_s\right)\nabla.\vec{u}_s \overline{\overline{I}} + \mu_s\left[\nabla \vec{u}_s + \left(\nabla \vec{u}_s\right)^T\right]$	(6)
Conservation of energy for gas and solids phases	$\frac{\partial}{\partial t}\left(\alpha_g \rho_g h_g\right) + \nabla.\left(\alpha_g \rho_g \vec{u}_g h_g\right) = -\alpha_g \frac{\partial p}{\partial t} + \nabla.\left(\alpha_g \kappa_g \nabla T_g\right) + \delta\left(T_s - T_g\right)$	(7)
	$\frac{\partial}{\partial t}\left(\alpha_s \rho_s h_s\right) + \partial.\left(\alpha_s \rho_s \vec{u}_s h_s\right) = -\alpha_s \frac{\partial p_s}{\partial t} + \nabla.\left(\alpha_s \kappa_s \nabla T_s\right) - \delta\left(T_s - T_g\right)$	(8)
	$h_i = \int_{T_{ref}}^{T} c_{p,i} dT$ with i = gas or solid	
Conservation of granular energy for solids phase	$0 = \left(-p_s \overline{\overline{I}} + \overline{\overline{\tau}}_s\right) : \nabla \vec{u}_s - \gamma_{\theta_s}$	(9)
	$\gamma_{\theta s} = \frac{12\left(1 - e_{ss}{}^2\right) g_o}{d_s \sqrt{\pi}} \rho_s \alpha_s{}^2 \theta_s{}^{3/2}$	(10)
	with $\vec{u}_s = \vec{u}_{s,mean} \pm \vec{u}'_s$ and $\theta_s = \frac{1}{3}\left(\vec{u}'_s.\vec{u}'_s\right)$	

Analogous to the thermodynamic temperature in gases, a granular temperature is defined, θ_s *(m^2/s^2),* which represents the fluctuating kinetic energy of the individual solid particles. The granular temperature is calculated based on a transport equation (Eq. 9), which assumes that the production of granular energy is balanced by its dissipation (Eq. 10) due to particle-particle collisions.

Closures for Momentum and Energy Conservation Equations

In order to close the momentum conservation equations for gas and solids phases, the solids-gas momentum exchange coefficient, solids phase viscosities and pressure have to be determined. In fluidized beds, the most important interaction force between the phases is the drag force. The gas-solid exchange coefficient due to drag force was calculated using an expression proposed by Syamlal and O'Brien [11] as shown in Eq. [11]. Once the granular temperature is obtained from Eq. 9, the kinetic theory relates μ_s, ζ_s and P_s to granular temperature, coefficient of restitution and radial distribution function. In this work, we use the kinetic theory model of Syamlal et al. [12]. In addition, gas phase turbulence is neglected.

In order to close the conservation of energy equations (Eqs. 7 and 8), the volumetric interphase heat transfer coefficient between gas and solids phases,δ, and the thermal conductivity of the solids phase, κ_s, should be modeled. FLUENT V6.2 uses the correlation of Gunn [13] for the gas-particle heat transfer coefficient as seen in Eq. 17 in Table 3. This correlation is valid for a wide range of particle volume fraction and models the convective heat transfer between the phases.

Table 2. Closure Equations – Conservation of Momentum

Solid-Gas momentum exchange coefficient [11]	$K_{gs} = \frac{3\alpha_s \alpha_g \rho_g}{4 v_{r,s}^2 d_s} C_D \left(\frac{Re_s}{v_{r,s}} \right) \left(\vec{u}_s - \vec{u}_g \right)$	(11)
	$C_D = \left(0.63 + \frac{4.8}{\sqrt{Re_s / v_{r,s}}} \right)^2$, $Re_s = \frac{\rho_g d_s \left\| \vec{u}_s - \vec{u}_g \right\|}{\mu_g}$	
	$v_{r,s} = 0.5 \left(A - 0.06\, Re_s + \sqrt{0.06\, Re_s^2 + 0.12\, Re_s (2B - A) + A^2} \right)$	
	$A = \alpha_g^{4.14}$, $B = 0.8 \alpha_g^{1.28}$ for $\alpha_g \le 0.85$, $B = \alpha_g^{2.65}$ for $\alpha_g > 0.85$	
Solids phase shear viscosity [12]	$\mu_{s,col} = \frac{4}{5} \alpha_s^2 \rho_s d_s g_{o,s} (1 + e_{ss}) \left(\frac{\theta_s}{\pi} \right)^{\frac{1}{2}}$	(12)
	$\mu_{s,kin} = \frac{\alpha_s d_s \rho_s \sqrt{\theta_s \pi}}{6(3 - e_{ss})} \left[1 + \frac{2}{5} (1 - e_{ss})(3 e_{ss} - 1) \alpha_s g_o \right]$	(13)
Solids phase bulk viscosity [12]	$\lambda_s = \frac{4}{3} \alpha_s^2 \rho_s d_s g_{o.s} (1 + e_{ss}) \sqrt{\frac{\theta_s}{\pi}}$	(14)
Solids phase pressure [12]	$p_s = \alpha_s \rho_s \theta_s + 2 \rho_s (1 + e_{ss}) \alpha_s^2 g_o \theta_s$	(15)
Radial distribution function [12]	$g_o = \frac{1}{1 - \alpha_s} + \frac{3 \alpha_s}{2 (1 - \alpha_s)^2}$	(16)

The conductivity of particle material, κ_{pm} differs from that of the solid phase, κ_s, which depends on the contact of the particles in a fluidized bed as seen in Fig 1. There are two main approaches in modeling the thermal conductivity of the solids phase [3, 4]. The first approach is based on the arrangement in a sphere packing and was originally developed by Zehner and Schlunder [6] to calculate the thermal conductivity of bulk solids phase as a function of the thermal properties of the gas and particle material, and void fraction. The second approach for modeling the solids phase thermal conductivity is based on kinetic theory of granular solids. Analogous to the kinetic theory of gases, kinetic theory of granular solids relate the thermal conductivity of the solids phase to the random particle fluctuations which is represented by granular temperature. Hsiau and Hunt [7] and Hunt [8] proposed a relation for the thermal conductivity of the solids phase as a function of granular temperature as given in Eq. 19 of Table 3.

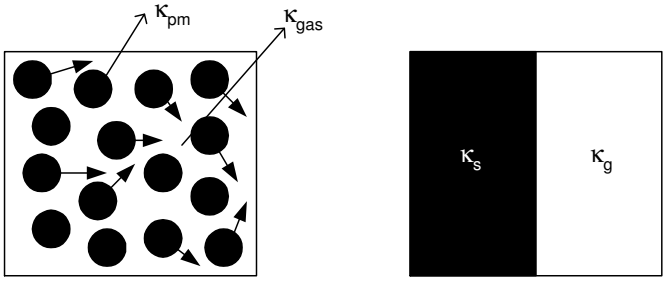

Figure 1. Concept of gas and particle phase thermal conductivities in TF approach, a) Thermal conductivities of the particle material and the gas, b) Modeled gas and solids phase thermal conductivities

Table 3. Closure Equations – Conservation of Energy

Volumetric interphase heat transfer coefficient	$\delta = \frac{6\kappa_s \alpha_g \alpha_s Nu_s}{d_s^2}$ where Nusselt number is given as [13] $Nu_s = \left(7 - 10\alpha_g + 5\alpha_g^2\right)\left(1 + 0.7\,Re_s^{0.2}\,Pr^{1/3}\right) + (1.33 - 2.4\alpha_g + 1.2\alpha_g^2)\,Re_s^{0.7}\,Pr^{1/3}$ (17)	
Thermal conductivity of the gas and solids phases – Non-kinetic theory approach [6]	$\alpha_s\kappa_s = \sqrt{1-\alpha_g}\left[\omega k_{pm} + (1-\omega)\kappa_{cyl}\right]$ $\alpha_g\kappa_g = \left(1 - \sqrt{1-\alpha_g}\right)\kappa_{gas}$ $\kappa_{cyl} = \frac{2\kappa_{gas}}{1 - \frac{\kappa_{gas}}{\kappa_{pm}}B}\left[\frac{\left(1 - \kappa_{gas}/\kappa_{pm}\right)B}{\left(1 - \left(\kappa_{gas}/\kappa_{pm}\right)B\right)^2} ln\frac{\kappa_{pm}}{B\kappa_{gas}} - \frac{B+1}{2} - \frac{B-1}{1 - \left(\kappa_{gas}/\kappa_{pm}\right)B}\right]$ $B = 1.25\left(\frac{1-\alpha_g}{\alpha_g}\right)^{10/9}$ and ω = 7.26 X 10^{-3}	(18)
Thermal Conductivity of the Solids Phase – Kinetic theory approach [7,8]	$\alpha_s\kappa_s = \alpha_s\rho_s c_{p,s} d_s \pi^{3/2}\frac{\sqrt{\theta}}{32 g_0}$ with $g_o = \frac{16 - 7\alpha_s}{16(1-\alpha_s)^2}$	(19)

Simulations

The simulations were carried out for a 2-D geometry, which has a width of 17 cm (the width of the bed is the same as the diameter of the Plexiglas bubbling fluidized bed as seen in Fig. 2b) and a height of 25 cm. In the experimental bubbling fluidized bed, a cylindrical cartridge heater with an outer diameter of 1.25 cm and a length of 2.54 cm was immersed horizontally at a height of 7 cm from the distributor plate to investigate the surface-to-bed heat transfer. The bed was initially filled with glass beads (150 μm, 2650 kg/m^3) to a height of 14.5 cm (identical to the static bed height in the experiments). The thermal conductivity and the heat capacity of the glass beads were 1.0 W/mK and 0.8 kJ/kgK, respectively. For this geometrical domain, two Cartesian grids with 7000 and 13000 cells were produced. The grid density was increased towards the heater surface since the HTC is known to be strongly dependant on the temperature gradient at the surface [1]. For 7000 cells, the individual cell sizes varied between 0.51 mm – 10 mm in ***x*** direction (spanwise) and 0.51 mm – 3.6 mm in ***y*** (streamwise) direction, respectively. For 13000 cells, these values were 0.3 mm – 6.25 mm (***x*** direction) and 0.3 mm – 2.9 mm (***y*** direction), respectively. The coefficient of restitution for particle-particle and particle-wall collisions was taken as 0.9. The simulations were transient and a time step of 0.001 s was used.

The walls of the fluidized bed and the heater surface were treated as no-slip surfaces for gas phase while the solids were allowed to slip. An average surface heat flux of 19.7 kW/m^2 was applied as a boundary condition at the heater surface, which was identical to the flux of the cartridge heater used in the experiments. Other walls of the bed were assumed to be non-conducting walls. The temperature of the inlet air and the initial bulk bed temperature (gas and solids) were assumed to be 20^{o}C. Similar to the experiments, the bulk bed temperature did not deviate from its initial value.

The heat transfer process was simulated up to 4.0 seconds of real time. This duration was found to be sufficient to track the formation, rise and bursting of bubbles as well as obtaining a time-averaged HTC between the heater surface and the bed. The time averaged HTC around the heater was calculated averaging the

instantaneous HTC values in the last second of the simulations. At the heater wall, the temperatures of the gas and solids are calculated using the prescribed heat flux:

$$q''_s = -\kappa_s \frac{\partial T_s}{\partial n}\Big|_w \text{ and } q''_g = -\kappa_g \frac{\partial T_g}{\partial n}\Big|_w \tag{20}$$

with $q'' = q''_s + q''_g$, where n is the normal direction to the wall. Then, the overall HTC is defined as:

$$h = \frac{q''}{(T_{wall} - T_{bed})} \tag{21}$$

where the temperature bed temperature can be calculated as:

$$T_{bed} = T_s \alpha_s + T_g \alpha_g \tag{22}$$

In Eq. (22), T_s and T_g are the temperatures of the gas and solids phases.

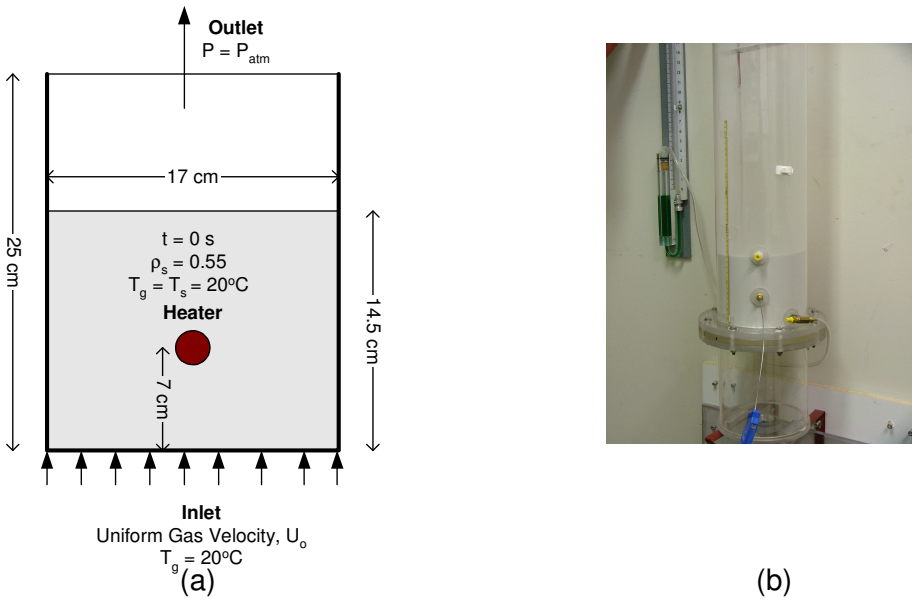

Figure 2. a) 2-D simulation geometry, b) Experimental set-up

Results and Discussion

Effect of Mesh Size on HTC

Fig. 3 shows the typical instantaneous volume fraction of solids around the heater for 7000 and 13000 cells at the same simulation conditions. The heater top surface is usually covered with solids phase with volume fractions close to maximum packing limit (stagnant solids with α_s ~ 0.6), whereas the sides and the bottom are shared with gas bubbles and the emulsion phase. For the finer mesh case (13000 cells), the size of the stagnant solids region is smaller. Fig. 4 presents the variation of the time averaged HTC around the heater for the same operating conditions. Although the variation of the HTC for both cases is similar, using a finer mesh increases the HTC. The low HTC values in the simulations are observed to correspond to the regions of stagnant solids or gas bubbles, which is consistent with the general theory of heat transfer in fluidized beds. Unfortunately, due to the limitation of the computational resources, the number of cells could not be increased beyond 13000.

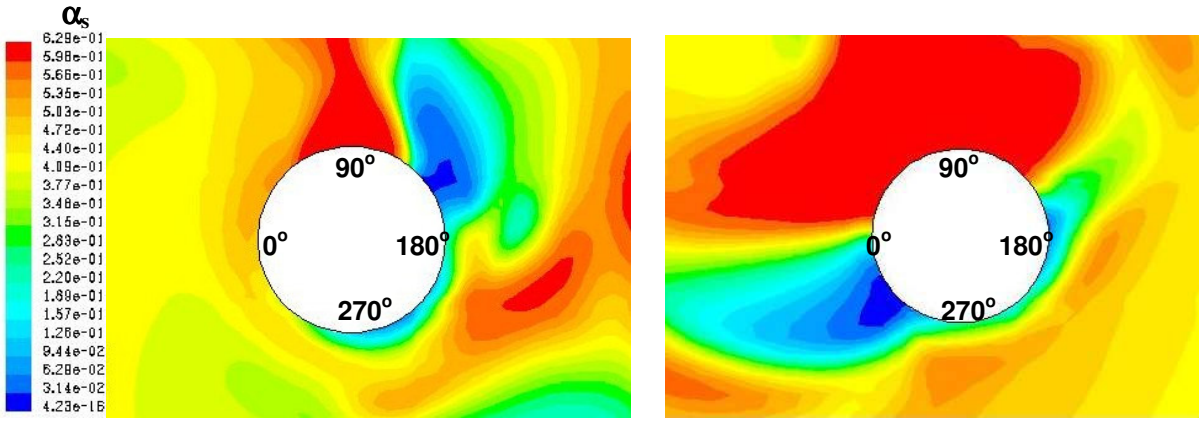

(a) 13000 cells (b) 7000 cells

Figure 3. Instantaneous volume fraction of solids at t = 4.0 s, U_0/U_{mf} = 3.33

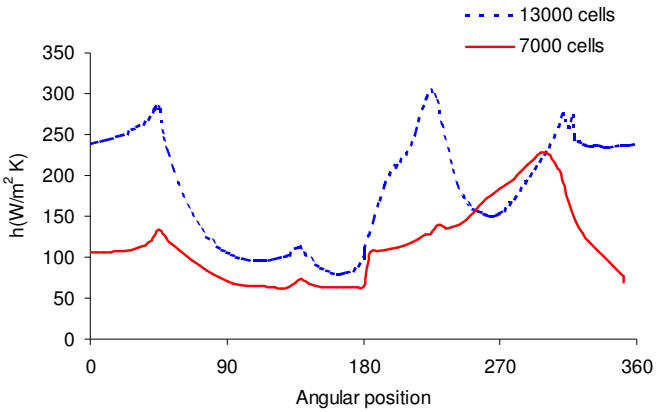

Figure 4. Effect of mesh size on time averaged HTC around the heater, U_0/U_{mf} = 3.33.

Effect of Solids Phase Thermal Conductivity Models on HTC

The effect of solids phase thermal conductivity models on HTC is shown in Fig. 5 with three different cases: 1) non-kinetic theory approach with κ_{pm} = 1 W/mK (glass bead thermal conductivity), 2) non-kinetic theory approach with κ_{pm} = 10 W/mK, 3) kinetic theory approach. The kinetic theory approach significantly overpredicts the experimental results, which is consistent with the simulations of Schmidt et al. [3, 4]. The kinetic theory approach also results in a marked decrease in heat transfer coefficient at the top of the heater where the solids phase is close to its maximum packing limit. With the non-kinetic theory approach, on the other hand, the experimental data is underpredicted. As the particle thermal conductivity, κ_{pm}, is increased ten folds (somewhat artificially for the sake of sensitivity analysis), the solids phase thermal conductivity, κ_s, increases and the simulated results approach to experimental values. These results can further be explained by investigating the solids phase conductivity values produced by each model as seen in Fig. 6.

Fig. 6 shows the comparison of effective solids phase thermal conductivity ($\alpha_s\kappa_s$) as calculated by kinetic and non-kinetic theory approaches for 150 μm glass bead particles. The kinetic theory approach is a strong function granular temperature (GT) and shows a peak around a solids volume fraction of 0.35. Non-kinetic theory approach results in increasing solids phase thermal conductivity with solids volume fraction possibly due to increasing particle-particle contacts. In this study, the granular temperature values for 150 μm glass bead particles varied between 10^{-4} –

10^{-3} in the simulations. This explains the higher HTC values produced by the kinetic theory approach. Furthermore, this also indicates the importance of accurately predicting the granular temperature distribution if the kinetic theory approach is to be used.

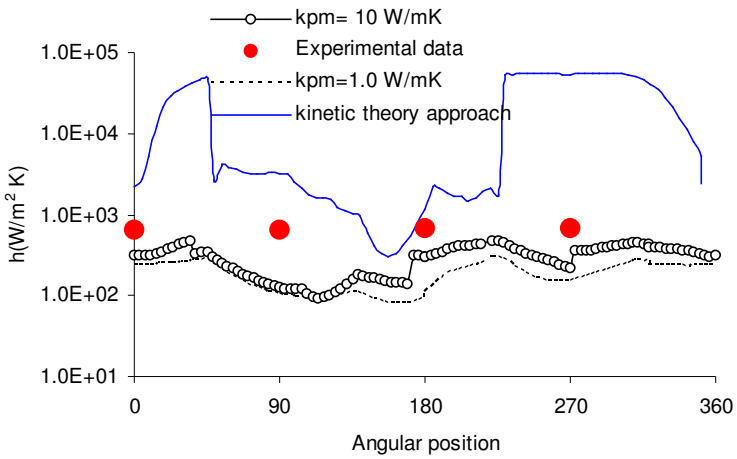

Figure 5. Effect of solids thermal conductivity models on time averaged heat transfer coefficient around heater, U_0/U_{mf} = 3.33, 13000 cells.

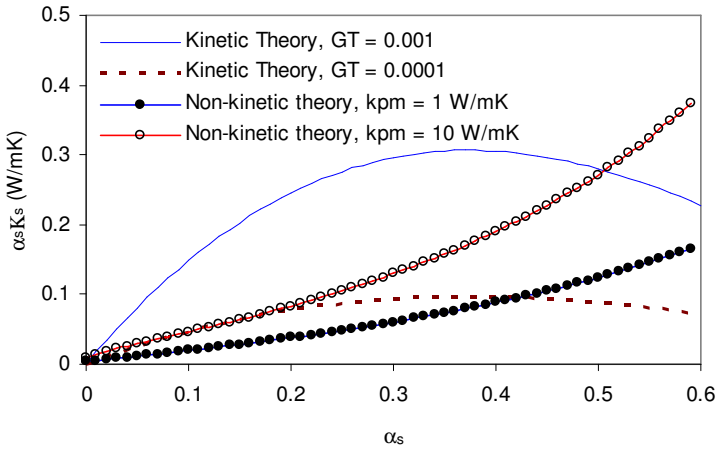

Figure 6. Comparison of kinetic theory and non-kinetic theory based approaches

Effect of Superficial Gas Velocity (U_o/U_{mf}) on HTC

Fig. 7 shows that the instantaneous solids volume fraction distribution at three different superficial gas velocities. The bed expands significantly as the superficial gas velocity is increased, decreasing the average solids volume fraction. As the bed becomes more agitated, solids mixing increases and the size of stagnant particle region at the top of the heater gets smaller. Fig. 8 compares the time averaged heat transfer coefficient obtained from the simulations with the experimental data. As the superficial gas velocity is increased beyond minimum fluidization velocity (in this case $U_{mf} \cong 3$ cm/s), the experimental data shows a steep increase in HTC due to increased particle contact at the heater surface. As U_o further increases, large bubbles inhibit the heat transfer due to their blanketing effect by covering the surface of the heater. For the simulation results, the bars indicate the variation of the HTC values around the heater for the given superficial gas velocity. The simulated HTC

increases from 182 W/m^{2}K at U_o/U_{mf} = 1.66 to 197 W/m^{2}K at U_o/U_{mf} = 3.33, which is the maximum value. It then decreases down to 121 W/m^{2}K at U_o/U_{mf} = 6.6. Therefore, although, the simulations underpredict the experimental HTCs, the experimental trend is somewhat captured.

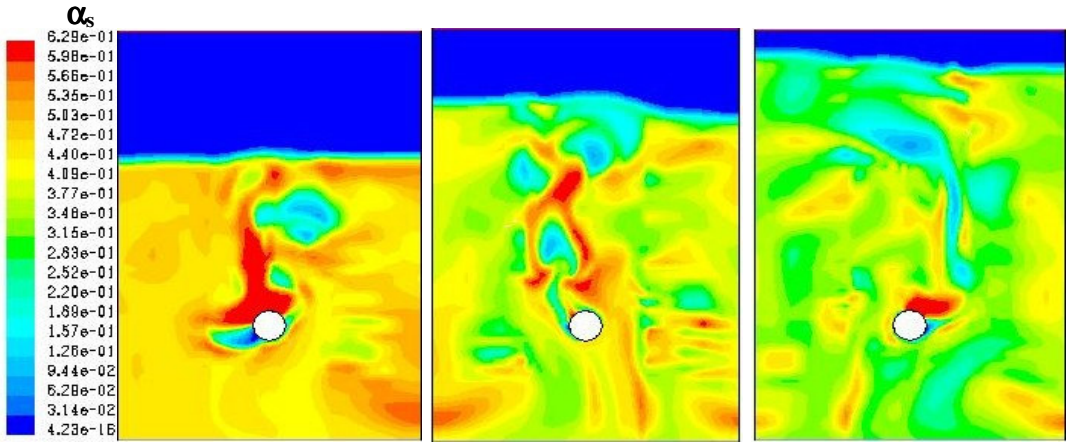

Figure 7. Instantaneous volume fraction of solids at t = 4.0 s, 13000 cells.

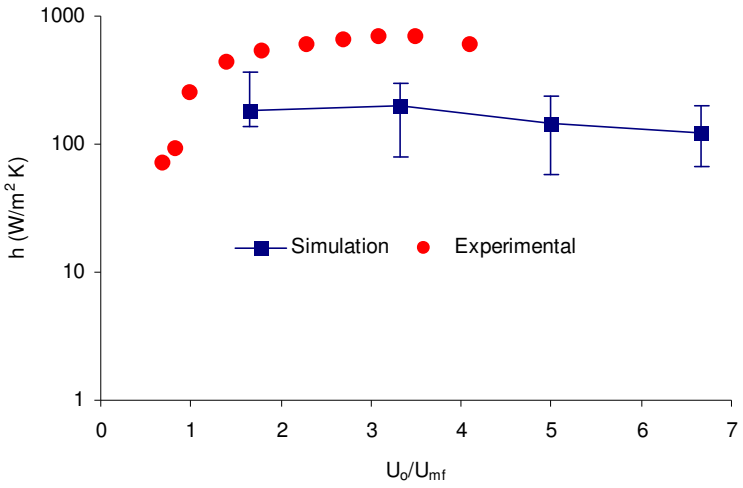

Figure 8. Comparison of the experimental and simulated time averaged HTCs, 13000 cells.

Effect of Coefficient of Restitution on HTC

In all simulations so far, the coefficient of restitution, which quantifies the elasticity of particle-particle collisions was taken as 0.9. The coefficient of restitution directly controls the dissipation of the granular energy (Eq. 10, Table 1), and is therefore an important parameter in the determination of the granular temperature distribution. Fig. 9 shows the effect of coefficient of restitution on time averaged HTC. As can be seen, as the coefficient of restitution increases from 0.9 to 1.0, the time averaged HTC also increases. When e_{ss} is set to 1.0, the granular energy is not dissipated leading to slightly higher granular temperature values in the bed. As the granular temperature is related to solids phase velocity fluctuations, higher HTC values with e_{ss} = 1.0 can be explained with improved solids phase-heater contact.

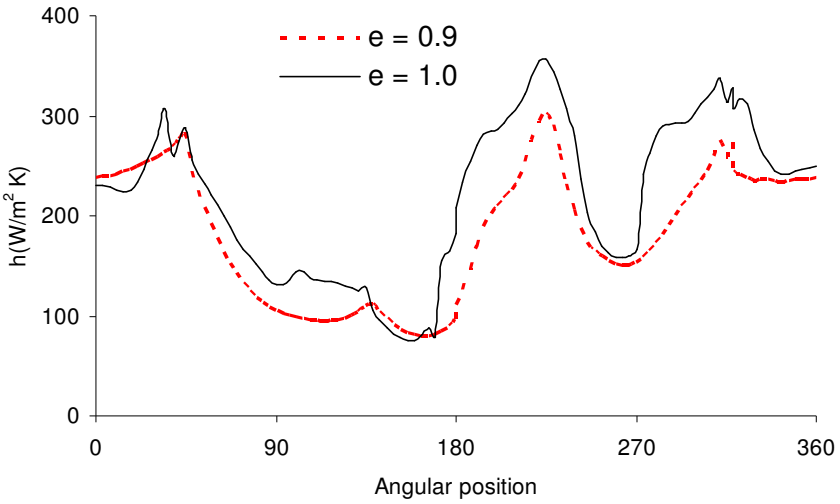

Figure 9. Effect of coefficient of restitution on time-averaged HTC around the heater, U_o/U_{mf} = 3.33, 13000 cells.

Conclusions

In this study, the surface-to-bed heat transfer in a freely bubbling fluidized bed was simulated numerically with TF approach coupled with kinetic theory of granular solids using a commercial software, FLUENT v6.2. The simulated results were compared with experimental measurements for validation. The conclusions obtained from this study can be summarized as follows:

The modeling of the solid phase thermal conductivity is a crucial part of heat transfer simulations in fluidized beds using TF approach. The kinetic theory approach [7,8] is a strong function of granular temperature and the simulated time averaged HTCs with this approach overpredict the experimental data. On the other hand, the so-called non-kinetic theory approach [3,4,6] results in underpredictions. The HTC is very sensitive to the mesh size at the heater surface. The coefficient of restitution, which is a parameter quantifying the elasticity of particle-particle collisions, is also found to affect the HTC. TF approach has been used in numerous studies in the past for hydrodynamic simulations in fluidized beds. Its application for heat transfer is promising, however, further research is necessary for better predictions quantitatively.

Acknowledgements

The authors would like to acknowledge NSERC (Natural Sciences and Engineering Research Council of Canada) for providing financial support for this work.

Nomenclature

d_s	particle diameter, m
g_o	radial distribution function, -
h	specific enthalpy, J/kgK
h	convective heat transfer coefficient, W/m^{2}K
K_{sg}	gas-solid momentum exchange coefficient, kg/m^{3}s
κ_{pm}	thermal conductivity of particle material, W/mK
κ_{gas}	thermal conductivity of gas, W/mK
κ_s	thermal conductivity of solid phase, W/mK

κ_{gas}	thermal conductivity of gas phase, W/mK
q''	heat flux, W/m^2
U_o, U_{mf}	superficial gas and minimum fluidization velocity, m/s
$\vec{u}$	velocity of gas or solid phases, m/s
$\vec{u}_s'$	fluctuating particle velocity, m/s
α	volume fraction of gas or solid phases, -
γ_{θ_s}	collisional dissipation of granular energy, m^2/s^2
δ	volumetric gas-solid heat transfer coefficient, W/m^{3}K
ζ_s	bulk viscosity of solid phase, kg/m.s
θ_s	granular temperature, m^2/s^2
μ_g	shear viscosity of gas phase, kg/m.s
μ_s	shear viscosity of solid phase, kg/m.s
ρ	density of gas or solid phases, kg/m^3
$\overline{\overline{\tau}}_g$	gas phase stress tensor, N/m^2
$\overline{\overline{\tau}}_s$	solid phase stress tensor, N/m^2

Literature

1. Syamlal, M., and Gidaspow, D (1985) Hydrodynamics of Fluidization: Prediction of Wall to Bed Heat Transfer Coefficients, *AIChE J.*, v. 31 (1), 12 7-13 5.
2. Kuipers, J. A. M., Prins, W. and Van Swaaij, W. P. M., (1992), Numerical Calculation of Wall-to-Bed Heat-Transfer Coefficients in Gas-Fluidized Beds, *AIChE J* , v. 38, 1079-1091.
3. Schmidt, A. and Renz, U., (1999), Eulerian Computation of Heat Transfer in Fluidized Beds", *Chemical Engineering Science,* v. 54, 5515-5522.
4. Schmidt, A. and Renz, U., (2000) Numerical Prediction of Heat Transfer in Fluidized Beds by a Kinetic Theory of Granular Flows, *Int. J. Thermal Science*., v. 39, 871-885.
5. Patil, D.J., Smit, J., van Sint, A., Kuipers, J.A.M., (2006), Wall-to-Bed Heat Transfer in Gas-Solid Bubbling Fluidized Beds", *AIChE J*, v.52, n.1., 58-74.
6. Zehner, P. and Schlunder, E.U., (1970), Warmeleitfahigkeit von Schuttungen Bei Mabigen Temperaturen, *Chernie Ing. Techn*. v. 42 (14), 933-941.
7. Hsiau, S. and Hunt M.L, (1993), Shear-Induced Particle Diffusion and Longitudinal Velocity Fluctuations in a Granular flow Mixing Layer, *J. Fluid Mech.*, v. 251, 299-313.
8. Hunt, M.L., (1997), Discreet Element Simulations for Granular Material Flows: Effective Thermal Conductivity and Self Diffusivity, *Int. J. of Heat and Mass Transfer*, v. 40 (13), 3059-3068.
9. Enwald, H., Peirano, E. and Almstedt, A.E. (1996), Eulerian Two-Phase Flow Applied to Fluidization, *Int. J. Multiphase Flow*, 22, 21-66.
10. Gidaspow, D., (1994) Multiphase Flow and Fluidization, Academic Press, London.
11. Syamlal, M. and O'Brien, T.J., (1989) Computer Simulation of Bubbles in a Fluidized Bed, *AIChE Symp. Series*, 85, 22-31.
12. Syamlal, M., O'Brien,T. J. and Rogers, W., (1993) MFIX Documentation: Volume 1, Theory Guide, National Technical Information Service, Springfield, V.A.
13. Gunn, D., (1978) Transfer of Heat or Mass to Particles in Fixed and Fluidized Beds, *Int. J. Heat Mass Transfer*, v. 21, 467-476.